American Mineralogist, Volume 65, pages 1185–1191, 1980

Cation vacancies and the crystal chemistry of breakdown reactions in kimberlitic omphacites

JOSEPH R. SMYTH

Geosciences Division, Los Alamos Scientific Laboratory
Los Alamos, New Mexico 87545

Abstract

The degree of alteration in clinopyroxenes from eclogitic inclusions in South African kimberlites is directly related to the deviation from stoichiometry of remnant unaltered areas in individual grains. Deviations from stoichiometry are reconciled by allowing up to 9 percent vacancy in the M2 site. The breakdown reaction accounting for the apparent alteration is:

$$Ca\,\square\,Al_2Si_4O_{12} \rightarrow CaAl_2SiO_6 + 3SiO_2$$

The products of this reaction are observed in X-ray precession photographs as a second Ca-Tschermak's pyroxene intergrown with the host omphacite plus quartz powder rings. I infer that a vacancy-containing pyroxene is stabilized by pressure but is highly unstable at lower pressures. A general FORTRAN program which breaks pyroxene compositions into end-members has been written to include a vacancy-containing end-member.

Introduction

In the course of mineralogical investigations of inclusions in South African kimberlite pipes, I noted that in eclogitic clinopyroxenes the apparent degree of breakdown closely correlates with the mineralogy of the specimen. Of the specimens observed, the kyanite- and coesite-bearing eclogites and grospydites exhibit the greatest degree of alteration, which appears as a cloudiness or white opacity in the clinopyroxenes. It is inferred that the alteration of these clinopyroxenes must have been extremely rapid and essentially isochemical, because coesite is preserved in one specimen in which the omphacitic pyroxene is quite altered (Smyth and Hatton, 1977; Smyth, 1977a). This led to the suspicion that a component in these pyroxenes is highly unstable at lower pressures, indeed much less stable than either jadeite or coesite.

In thin section, the alteration of the pyroxene appears fairly evenly distributed along very fine fractures (Fig. 1); however, small unaltered areas up to 50 μm in diameter remain throughout most grains. Also, the pyroxene appears unaltered where it occurs as inclusions up to 200 μm in diameter within coesite and garnet grains. Preliminary microprobe analyses of the unaltered areas showed that the pyroxenes contained Al^{VI} significantly in excess of Al^{IV} + Na + K, and had consistently and significantly fewer than 8.0 cations per 12.0 oxygens. A similar deviation from stoichiometry was noticed by Sobolev *et al.* (1968) in omphacites in kyanite eclogites from Siberian kimberlites, although no explanation was offered as to how such deviations might be maintained. O'Hara and Yoder (1967) reported anomalously high alumina in pyroxenes synthesized at 1500°C and 3.0 GPa (30 kbar), and suggested that there may be a solid solution toward kyanite. Thus, previous studies and the preliminary chemical data suggest that the deviations from stoichiometry might be responsible for the rapid breakdown of some of the omphacites, especially those from kyanite- and silica-bearing eclogites.

Wood and Henderson (1978) presented experimental evidence for substantial amounts of M-site vacancies in aluminous clinopyroxenes in the systems $CaAl_2SiO_6$–SiO_2 and $CaAl_2SiO_6$–$CaMgSi_2O_6$ at pressures of 25–32 kbar and temperatures of 1400–1500°C. They concluded that the non-stoichiometric pyroxene is stabilized by increased pressure and should be a stable component of natural clinopyroxenes, especially in the presence of excess SiO_2. My investigation was undertaken to document the existence and extent of the occurrence of vacancies in some natural jadeite-rich clinopyroxenes and to characterize the crystal chemistry of the breakdown

0003–004X/80/1112–1185$02.00

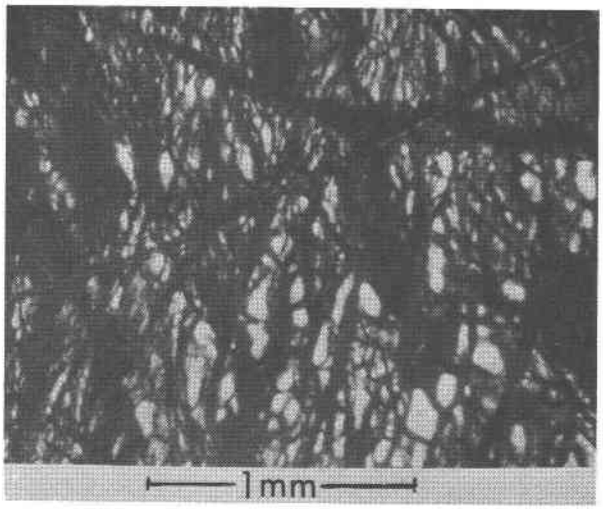

Fig. 1. Transmitted light photograph (crossed polars) of alteration in a single grain of clinopyroxene from sample SRV-1, a coesite grospydite.

reactions of the non-stoichiometric end-member. Such a study should facilitate understanding and recognition of these minerals and may lead to a further definition of the *P–T* stability field of these clinopyroxenes in Na-bearing systems by experimental methods.

Chemistry

Mantle-derived eclogites, unlike peridotites and lherzolites, contain significant amounts of phases that typically break down at lower pressures. Consequently, these phases must be brought to the surface and quenched rapidly in order to be preserved, and the most common near-surface occurrence is as inclusions in kimberlite pipes. In such pipes, peridotites and lherzolites generally predominate over eclogites by an estimated 20:1 (Harte and Gurney, 1975). However, in a few pipes such as Roberts Victor in South Africa and Zagodochnaya in Siberia, eclogites predominate over other types of inclusions and provide an unusual range of eclogite compositions. Relatively few (<150) major-element chemical analyses of the principal minerals of these rocks exist in the literature and very few are from kyanite eclogites and grospydites (Sobolev *et al.*, 1968; Kushiro and Aoki, 1968; Mathias *et al.*, 1970; MacGregor and Carter, 1970; Lappin and Dawson, 1975; Harte and Gurney, 1975; Reid *et al.*, 1976; Lappin, 1978; Hatton and Gurney, 1979; Shee and Gurney, 1979). The clinopyroxenes in these rocks range in composition from about $Jd_5Di_{80}Hd_{15}$ to $Jd_{70}Di_{25}Hd_5$. Of the reported analyses of clinopyroxenes from kimberlitic eclogites, more than 70 percent show an excess of $Fe^{3+} + Al^{VI}$ over $Al^{IV} + Na + K$ and calculated cation totals of significantly fewer than 8.0 per 12 oxygens. All of those from grospydites and kyanite eclogites show a substantial excess of Al^{VI}.

Table 1 gives microprobe chemical analyses of ten clinopyroxenes from kimberlite inclusions, including two eclogites, one rutile eclogite, three kyanite eclogites, and four silica–kyanite eclogites. Eight samples are from Roberts Victor and the other two from nearby kimberlite pipes. All analyses show a significant excess of octahedrally-coordinated Al over $Al^{IV} + Na + K$ and significantly fewer than 8.0 cations per 12 oxygens. In these analyses, total Fe is reported as Fe^{2+}. If ferric iron is present, as indicated in wet-chemical analyses of similar samples (Kushiro and Aoki, 1968; Sobolev *et al.*, 1968), the apparent cation deficiency would be increased. All analyses in Table 1 indicate nearly enough silica to fill the tetrahedral site, so that there is relatively little Al^{IV} and the excess of Al cannot be ascribed to Ca-Tschermak's (CaTs) molecule. The calculated cation ratios indicate a deficiency of cations such that the pyroxene structure can be maintained only by the inclusion of a significant portion of M-site vacancies.

The stoichiometry of these pyroxenes can best be reconciled if the hypothetical end-member $Ca_{0.5}\square_{0.5}AlSi_2O_6$ is considered (where $\square$ is a vacancy). This end-member was first hypothesized by Vogel (1966), based on the need to explain isochemical symplectitic breakdown of omphacites to diopside plus feldspar. There is some liberty in choosing such an end-member, but the rules for assigning cations to sites in pyroxenes are fairly restrictive. The radius of the octahedral Al is small enough to be restricted to the M1 site and Ca is the logical choice as a divalent cation restricted to M2. Ferrous iron or magnesium can be used if there is a deficiency of Ca, but such a case has not yet come to light. Although there is no reason to assume that the vacancies are restricted to M2, it seems likely that most of them are in M2 because of the known site preferences of the remaining cations. Wood and Henderson (1978) report evidence for vacancies in both M1 and M2, with the latter predominating.

Breakdown reactions

Further evidence for the existence of M-site vacancies comes from a study of the breakdown reactions in some pyroxenes. Sample SRV-1, a coesite grospydite described by Smyth and Hatton (1977),

Table 1. Electron microprobe chemical analyses of peraluminous omphacites

	1 SRV-1	2 SRV-6	3 SRV-7	4 SRV-8	5 SRV-9	6 SRV-10	7 SRV-12	8 SRV-20	9 SBB-1	10 SFS-1
Oxide Weight Percents										
SiO_2	55.6	57.3	56.0	57.8	56.4	56.9	56.2	56.3	56.9	56.1
TiO_2	.1	.4	.2	.4	.4	.3	.3	.4	.4	.4
Al_2O_3	17.2	17.2	15.6	17.1	16.1	16.7	14.0	13.3	19.4	16.1
Cr_2O_3	.04	.03	.06	.08	.04	.07	.09	.2	.01	.05
FeO	1.7	2.0	1.4	1.6	2.2	2.0	2.4	2.6	2.5	2.4
MnO	.05	.00	.04		.06		.04	.06	.07	.03
MgO	6.2	5.3	7.5	6.4	7.1	6.5	8.3	8.4	4.1	6.5
CaO	11.7	11.0	12.0	9.7	9.8	10.6	11.8	12.1	7.7	10.7
Na_2O	6.8	7.3	6.6	8.3	7.4	7.9	6.9	6.6	9.1	7.6
K_2O	.2	.2	.2	.2	.1	.1	.2	.2	.1	.1
Total	99.6	100.7	99.6	101.6	99.6	101.1	100.1	99.9	100.2	99.6
Cations per 12 Oxygens										
Si	3.88	3.95	3.92	3.94	3.93	3.92	3.94	3.95	3.92	3.92
Al^{IV}	.12	.05	.08	.06	.07	.08	.06	.05	.08	.08
Al^{VI}	1.30	1.35	1.20	1.32	1.25	1.27	1.09	1.05	1.50	1.24
Ti	.01	.02	.01	.02	.02	.02	.02	.02	.02	.02
Cr	.00	.00	.00	.00	.00	.00	.01	.01	.00	.00
Fe^{2+}	.10	.11	.08	.09	.13	.11	.14	.15	.14	.14
Mn	.00	.00	.00		.00		.00	.00	.00	.00
Mg	.65	.55	.78	.65	.74	.67	.86	.88	.42	.67
Ca	.87	.81	.90	.71	.73	.78	.88	.91	.57	.80
Na	.92	.97	.89	1.10	1.00	1.05	.94	.89	1.22	1.03
K	.02	.02	.02	.02	.01	.01	.01	.01	.01	.01
Total	7.87	7.83	7.87	7.91	7.88	7.91	7.95	7.92	7.88	7.92

1.	Coesite grospydite	Roberts Victor
2.	Coesite grospydite	Roberts Victor
3.	Coesite grospydite	Roberts Victor
4.	Kyanite eclogite	Roberts Victor
5.	Rutile eclogite	Roberts Victor
6.	Kyanite eclogite	Roberts Victor
7.	Eclogite	Roberts Victor
8.	Coesite eclogite	Roberts Victor
9.	Kyanite eclogite	Babejaan
10.	Eclogite	Frank Smith

provides useful control on the reaction types and rates. The preservation of coesite in the sample indicates that it did not spend more than a few hours above about 600°C after crossing into the pressure stability field of quartz. Because of the presence of unaltered kyanite, garnet, and sanidine in the rock and the existence of coesite, it is unlikely that there was significant loss of any cations (*e.g.*, Rb, K, Na), so the reactions may be assumed to be essentially isochemical. Further, microprobe analyses of unaltered omphacite inclusions in kyanite and coesite do not differ significantly from those of apparently altered areas.

X-ray precession photographs (Fig. 2) of the altered clinopyroxene in this sample indicate the presence of two pyroxenes of distinctly different compositions plus non-oriented polycrystalline quartz. All the powder rings on these photographs can be accounted for by quartz, and there is no evidence of exsolved coesite. Despite the substantial mosaicity (seen in all exsolved crystals X-rayed) the general axial relationships between host and lamellae seen in

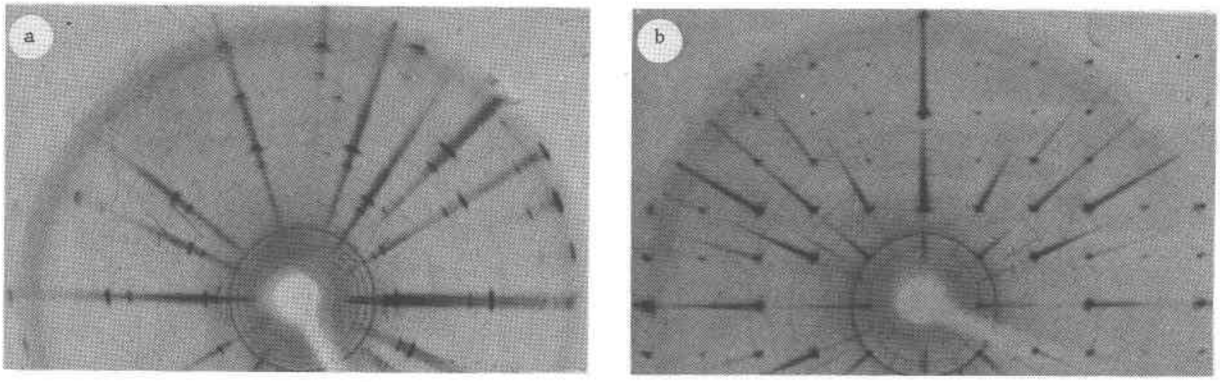

Fig. 2. (a) *b*-axis precession photograph (c^* horizontal, zero-level unfiltered Mo radiation) of omphacite from coesite grospydite SRV-1. This photograph shows two pyroxenes of differing a^* (lengths and direction) and nearly common c^*. Also apparent are powder diffraction rings from non-oriented microcrystalline quartz. (b) *a*-axis precession photograph (b^* horizontal, zero-level, Zr-filtered Mo radiation) of the same crystal. This photograph shows the two pyroxenes of differing b^* and apparently common c^*. Quartz powder rings are also present.

Figure 2 are:

$a_l \neq a_h$ a_l not parallel a_h

$b_l \neq b_h$ b_l approx. parallel b_h

$c_l \cong c_h$ c_l approx. parallel c_h

The above relationships indicate a radically different geometry of exsolution than has been observed in the Ca–Mg–Fe pyroxenes (*cf.* Robinson *et al.*, 1977). In the quadrilateral pyroxenes, the host and lamellae all share nearly parallel and equal *b* axes. In the omphacite described here, the host and lamellae appear to share a nearly common *c* axis, while substantial differences occur along *a* and *b*. Such differences could be accommodated by lamellae lying in the [001] zone, perhaps near (110), although precise determination of exsolution geometry is the subject of a further study by transmission electron microscopy.

Cell parameters of the two phases were determined by least-squares refinement of manual centering parameters of ten strong reflections in a four-circle goniostat using Mo$K\alpha_1$ radiation (Table 2). Cell parameters of the host are consistent with a jadeite-rich omphacite, while those of the lamellae are consistent with a strained diopside or CaTs-rich diopside (Clark *et al.*, 1969; Okamura *et al.*, 1974). The reaction which has given rise to the lamellae is probably of the type:

$$Ca\square Al_2Si_4O_{12} \rightarrow CaAlAlSiO_6 + 3SiO_2$$

where diopside and jadeite components may partition between the two pyroxene components. The fact that the silica is quartz is evidence that the reaction occurred on eruption.

Pyroxene stoichiometry and end-member calculations

The existence of vacancies in natural kimberlitic omphacites introduces an additional variable into calculations of pyroxene end-members and proportions of Fe^{2+} to Fe^{3+} determined from microprobe chemical analyses. This means that it is impossible to calculate the Fe^{2+}/Fe^{3+} ratio from stoichiometric considerations (*e.g.*, Essene and Fyfe, 1967; Råheim and Green, 1975; Ryburn *et al.*, 1976; Mysen and Griffin, 1973; Hamm and Vieten, 1971; Cawthorne and Collerson, 1974) if substantial numbers of vacancies exist in the structure. The effect of the vacancies on Råheim and Green's geothermometer is to reduce the apparent temperature calculated from the Fe–Mg distribution coefficient between coexisting

Table 2. Cell parameters of host and exsolved pyroxene phases in sample SRV-1

	Host	Exsolved
a (Å)	9.553 (9)	9.671 (13)
b (Å)	8.694 (10)	8.849 (14)
c (Å)	5.231 (5)	5.264 (7)
β (°)	107° 10' (5')	106° 30' (5')
Vol (Å^3)	415.1	432.0
Space Group	C 2/c	C 2/c

garnet and clinopyroxene if the Fe^{2+}/Fe^{3+} ratio is calculated from microprobe chemical analyses. This may not be too serious, because there is evidence for vacancies only in silica- and alumina-rich kimberlitic eclogites, and the stoichiometric methods of estimating Fe_2O_3 contents of most clinopyroxenes are probably valid. However, the extent of the occurrence of vacancies in omphacites is not known and certainly warrants further experimental investigation.

Program description: table of end-members

A FORTRAN code[1] has been developed for the calculation of pyroxene end-members and Fe^{2+}–Fe^{3+} ratios. The end-member calculations are based upon the method of Ross (1976, unpublished), with several modifications. First, the Fe^{2+}–Fe^{3+} ratio is determined from stoichiometry by the method of Ryburn *et al.* (1976). If all Fe calculates as Fe^{2+} and a deficiency of cations per 6 oxygens still exists, the program assumes M-site vacancy. If all Fe calculates as Fe^{3+} and an excess of cations per 6 oxygens remains, the program indicates an error. Only Al and Si are permitted in the T sites. Al^{VI} is then determined by subtracting Al^{IV} from total Al. Negative amounts of Al^{IV} or Al^{VI} are then interpreted as an error. The current version of the code does not consider Ti^{3+} or allow Fe^{3+} in the T site, although these can easily be added. The sequence of end-member calculation is given in Table 3.

The program accepts cation numbers or weight percent oxides as input, and outputs weight and mole percents of only the end-members present. The program is written to be operable under Digital Equipment Corporation's RT-11 system which is commonly used in electron microprobe automation systems. Copies of the program are also available on DEC-compatible flexible disks from the author.

Table 3. Sequence of end-member removal

Sequence No.	End-Member	Sequence No.	End-Member
(1) $Li\ R^{3+}\ Si_2O_6$		(8) $R^{2+}\ Cr^{3+}\ AlSiO_6$	
a	$Li\ Cr\ Si_2O_6$	a	$Ca\ Cr\ AlSiO_6$
b	$Li\ Fe\ Si_2O_6$	b	$Mg\ Cr\ AlSiO_6$
c	$Li\ Al\ SiO_6$	c	$Fe\ Cr\ AlSiO_6$
(2) $Li\ R^{2+}_{.5}\ Ti^{4+}_{.5}\ Si_2O_6$		(9) $R^{2+}\ Fe^{3+}\ AlSiO_6$	
a	$Li\ Mg_{.5}Ti_{.5}\ Si_2O_6$	a	$Ca\ Fe\ AlSiO_6$
b	$Li\ Fe_{.5}Ti_{.5}Si_2O_6$	b	$Mg\ Fe\ AlSiO_6$
		c	$Fe\ Fe\ AlSiO_6$
(3) $Na\ R^{3+}\ Si_2O_6$		(10) $R^{2+}\ Al\ AlSiO_6$	
a	$Na\ Cr\ Si_2O_6$	a	$Ca\ Al\ AlSiO_6$
b	$Na\ Fe\ Si_2O_6$	b	$Mg\ Al\ AlSiO_6$
c	$Na\ Al\ Si_2O_6$	c	$Fe\ Al\ AlSiO_6$
(4) $Na\ R^{2+}_{.5}\ Ti^{4+}_{.5}\ Si_2O_6$		(11) $R^{2+}_{.5}\ Al\ Si_2O_6$	
a	$Na\ Mg_{.5}\ Ti_{.5}\ Si_2O_6$	a	$Ca_{.5}\ AlSi_2O_6$
b	$Na\ Fe_{.5}\ Ti_{.5}\ Si_2O_6$	b	$Mg_{.5}\ AlSi_2O_6$
		c	$Fe_{.5}\ AlSi_2O_6$
(5) $K\ R^{3+}\ Si_2O_6$		(12) $R^{2+}\ Mn\ Si_2O_6$	
a	$K\ Cr\ Si_2O_6$	a	$Ca\ Mn\ Si_2O_6$
b	$K\ Fe\ Si_2O_6$	b	$Mn\ Mg\ Si_2O_6$
c	$K\ Al\ Si_2O_6$	c	$Mn\ Fe\ Si_2O_6$
(6) $K\ R^{2+}_{.5}\ Ti^{4+}_{.5}\ Si_2O_6$		(13) $R^{2+}_2\ Si_2O_6$	
a	$K\ Mg_{.5}Ti_{.5}\ Si_2O_6$	a	$Ca_2\ Si_2O_6$
b	$K\ Fe_{.5}\ Ti_{.5}\ Si_2O_6$	b	$Mg_2\ Si_2O_6$
		c	$Fe_2\ Si_2O_6$
(7) $R^{2+}\ Ti^{4+}\ Al_2O_6$			
a	$Ca\ Ti\ Al_2O_6$		
b	$Mg\ Ti\ Al_2O_6$		
c	$Fe\ Ti\ Al_2O_6$		

End-member calculations for the ten omphacites in Table 1 are given in Table 4. All calculations resulted in negligible (<0.1%) residuals (cations not assignable to an end-member). Table 4 shows that in all cases the vacancy end-member, $Ca_{0.5}\square_{0.5}AlSi_2O_6$, is a very significant component. Calculations according to this scheme were performed on many published analyses of omphacites from kimberlite localities and the vacancy end-member was found to be significant (>2%) in more than half of these analyses. The end-member was not found to be a significant component of any other pyroxenes tested.

Conclusions

Chemical analyses indicate that vacancies are significant in the M-sites of omphacitic clinopyroxenes from kimberlite inclusions. The chemistry and crystallography of the breakdown products indicate that the reaction, $2\ Ca_{0.5}\square_{0.5}AlSi_2O_6 \rightarrow CaAlAlSiO_6 + 3SiO_2$ accounts for the whitish alteration apparent in the more silica-rich eclogites. I infer that the vacancies are stabilized by pressures in excess of 3.0 GPa but are highly unstable at lower pressures.

---

[1] To receive a copy of this program, order Document AM-80-143 from the Business Office, Mineralogical Society of America, 2000 Florida Avenue, N.W., Washington, D.C. 20009. Please remit $1.00 in advance for the microfiche.

Table 4. End-member calculations for kimberlitic omphacites (mole %)

	SRV 1	SRV 6	SRV 7	SRV 8	SRV 9	SRV 10	SRV 12	SRV 20	SBB 1	SFS 1
$NaCrSi_2O_6$	0.1	0.1	0.2	0.2	0.1	0.2	0.2	0.6	0.0	0.1
$NaAlSi_2O_6$	45.8	47.6	44.5	54.7	49.9	52.5	46.5	44.3	60.8	51.3
$KAlSi_2O_6$	0.9	0.9	0.9	0.9	0.4	0.4	0.9	0.9	0.4	0.4
$CaTiAl_2O_6$	0.3	1.0	0.5	1.0	1.0	0.8	0.8	1.0	1.0	1.1
$CaAlAlSiO_6$	5.3	0.6	3.3	0.9	1.3	2.6	1.9	0.6	1.8	2.1
$\square_{0.5}Ca_{.5}AlSi_2O_6$	12.9	17.0	11.2	9.4	11.1	8.1	4.9	6.5	11.8	8.1
$CaMnSi_2O_6$	0.1		0.1	-	0.2	-	0.1	0.2	0.2	0.1
$Ca_2Si_2O_6$	15.8	15.2	17.7	14.4	14.3	15.9	19.5	20.2	9.7	16.3
$Mg_2Si_2O_6$	16.1	13.6	19.5	16.3	18.5	16.7	21.6	21.9	10.5	16.9
$Fe_2Si_2O_6$	2.5	2.9	2.0	2.3	3.2	2.9	3.5	3.8	3.6	3.5

A FORTRAN code has been developed to include vacancy in pyroxene end-member calculations from microprobe or other chemical analyses. Calculations on a wide variety of pyroxenes indicate vacancy end-members may comprise up to 17% of kimberlitic omphacites but are not significant in pyroxenes from other petrogeneses.

Acknowledgments

This work was supported by the U.S. Department of Energy, Office of Basic Energy Sciences, and performed at Los Alamos Scientific Laboratory, which is operated by the University of California under contract W-7405-ENG-36.

References

Cawthorne, W. G. and K. D. Collerson (1974) The recalculation of pyroxene end-member parameters and the estimation of ferrous and ferric iron content from electron microprobe analyses. *Am. Mineral., 59,* 1203–1208.

Clark, J. R., D. E. Appleman and J. J. Papike (1969) Crystal-chemical characterization of clinopyroxenes based on eight new structure refinements. *Mineral. Soc. Am. Spec. Pap., 2,* 31–50.

Essene, E. and W. S. Fyfe (1967) Omphacite in Californian metamorphic rocks. *Contrib. Mineral. Petrol., 15,* 1–23.

Hamm, H. M. and K. Vieten (1971) Zur Berechnung der Kristallchemischen Formel und des Fe^{3+} Gehaltes von Klinopyroxen aus Electronenstrahl-Microanalysen. *Neues Jahrb. Mineral. Monatsh.,* 310–314.

Harte, B. and J. J. Gurney (1975) Evolution of clinopyroxene and garnet in an eclogite nodule from the Roberts Victor kimberlite pipe, South Africa. *Phys. Chem. Earth, 9,* 367–387.

Hatton, C. J. and J. J. Gurney (1979) A diamond–graphite eclogite from the Roberts Victor Mine. *Proc. Second Int. Kimberlite Conf., 2,* 29–36.

Kushiro, I. and K. Aoki (1968) Origin of some eclogite inclusions. *Am. Mineral., 53,* 1347–1367.

Lappin, M. R. (1978) The evolution of a grospydite from the Roberts Victor Mine, South Africa. *Contrib. Mineral. Petrol., 66,* 221–241.

——— and J. B. Dawson (1975) Two Roberts Victor cumulate eclogites and their reequilibration. *Phys. Chem. Earth, 9,* 351–365.

MacGregor, I. D. and J. L. Carter (1970) The chemistry of clinopyroxenes and garnets of eclogite and peridotite xenoliths from the Roberts Victor Mine, South Africa. *Phys. Earth. Planet. Interiors, 3,* 391–397.

Mathias, M., J. C. Siebert and P. C. Rickwood (1970) Some aspects of the mineralogy and petrology of ultramafic xenoliths in kimberlite. *Contrib. Mineral. Petrol., 26,* 75–123.

Mysen, B. and W. L. Griffin (1973) Pyroxene stoichiometry and the breakdown of omphacite. *Am. Mineral., 53,* 60–63.

O'Hara, M. J. and H. S. Yoder (1967) Formation and fractionation of basic magmas at high pressures. *Scottish J. Geol., 3,* 67–117.

Okamura, F. P., S. Ghose and H. Ohashi (1974) Structure and crystal chemistry of calcium Tschermak's pyroxene, $CaAlAlSiO_6$. *Am. Mineral., 59,* 549–557.

Råheim, A. and D. H. Green (1975) *P–T* paths of natural eclogites during metamorphism—a record of subduction. *Lithos, 8,* 317–378.

Reid, A. M., R. W. Brown, J. B. Dawson, G. G. Whitfield and J. C. Siebert (1976) Garnet and pyroxene compositions in some diamondiferous eclogites. *Contrib. Mineral. Petrol., 58,* 203–220.

Robinson, P., M. Ross, G. L. Nord, Jr., J. R. Smyth and H. W. Jaffe (1977) Exsolution lamellae in augite and pigeonite: fossil indicators of lattice parameters at high temperature and pressure. *Am. Mineral., 62,* 857–873.

Ryburn, R. J., A. Råheim and D. H. Green (1976) Determination of the *P–T* paths of natural eclogites during metamorphism—a record of subduction. A correction to a paper by Råheim and Green (1975). *Lithos, 9,* 161–164.

Shee, S. R. and J. J. Gurney (1979) The mineralogy of xenoliths from Orapa, Botswana. *Proc. Second Int. Kimberlite Conf., 2,* 37–49.

Smyth, J. R. (1977a) Peraluminous omphacite: cation vacancies in mantle-derived pyroxene (abstr.). *Trans. Am. Geophys. Union, 58,* 523.

——— (1977b) Quartz pseudomorphs after coesite. *Am. Mineral., 62,* 828–830.

——— and C. J. Hatton (1977) A coesite–sanidine grospydite from the Roberts Victor kimberlite. *Earth Planet. Sci. Lett., 34,* 284–288.

Sobolev, N. V., Jr., I. K. Kuznetsova and N. I. Zyuzin (1968) The petrology of grospydite xenoliths from the Zagodochnaya kimberlite pipe in Yakutia. *J. Petrol., 9,* 253–280.

Vogel, D. E. (1966) Nature and chemistry of the formation of clinopyroxene–plagioclase symplectite from omphacite. *Neues Jahrb. Mineral. Monatsh.,* 185–189.

Wood, B. J. and C. M. B. Henderson (1978) Composition and unit cell parameters of synthetic non-stoichiometric tschermakitic clinopyroxenes. *Am. Mineral., 63,* 66–72.

Manuscript received, June 25, 1979;
accepted for publication, June 15, 1980.